ELSEVIER

Spectrochimica Acta Part A 58 (2002) 1329–1335

SPECTROCHIMICA ACTA PART A

www.elsevier.com/locate/saa

Filling factor in a pulsed electron paramagnetic resonance experiment

Aharon Blank, Haim Levanon *

Department of Physical Chemistry and the Farkas Center for Light-Induced Processes, The Hebrew University of Jerusalem, 91904 Jerusalem, Israel

Received 1 July 2001; accepted 1 October 2001

Abstract

A definition and mathematical treatment to calculate the filling factor in a pulsed electron paramagnetic resonance (EPR) experiment are presented. The differences between filling factors in traditional, continuous wave (CW)-EPR experiments (η), and in pulsed-EPR experiments (η_p), are discussed. We present some examples to demonstrate how η_p depends upon the particular pulse sequence and sample characteristics. © 2002 Elsevier Science B.V. All rights reserved.

Keywords: EPR; Filling factor; FT-EPR; Time resolved EPR

1. Introduction

The term 'filling factor' in CW-electron paramagnetic resonance (EPR) measurements was introduced by Feher [1]. It relates the EPR signal intensity with the sample geometry and dielectric properties. Knowledge of the filling factor of a certain sample inside a specific cavity is important in many aspects of EPR spectroscopy. The general description given for calculating the filling factor in a CW-EPR experiment is [1]:

$$\eta = \frac{\int_{V_s} H_I^2 \, dV}{\int_{V_c} H_I^2 \, dV}, \quad (1)$$

where H_I is the microwave field intensity, V_s is the sample volume and V_c is the cavity volume. Having calculated the filling factor of a sample, we can estimate its EPR signal intensity, S_{EPR}, via the relation:

$$S_{EPR} \propto \chi'' \eta Q_L, \quad (2)$$

where Q_L is the quality factor of the loaded cavity, χ'' is the sample susceptibility and η can be estimated via Eq. (1) quite accurately. It is easy to calculate η if we assume that the inserted sample does not perturb the magnetic fields in the cavity. In such a case, one can use the analytical expressions of the fields inside the cavity [2]. It is obvious, however, that in most cases this approximation is oversimplified and is not accurate. In other words, η should be calculated under conditions where the fields in the cavity change upon sample insertion. Thus, one should compensate

* Corresponding author. Tel.: +972-2-658-5544; fax: +972-2-561-8033.

E-mail address: levanon@chem.ch.huji.ac.il (H. Levanon).

1386-1425/02/$ - see front matter
PII: S1386-1425(01)00722-3

the analytical expression for η by semi-empirical methods [3,4], or by calculating the fields' distribution by numerical calculations [5]. In terms of Eq. (2), it is evident that η is very important with respect to the signal-to-noise ratio [1], optimal sample size [1,2], and quantitative measurements of the number of spins in a given sample [5–7]. Despite the increase in EPR data employing pulsed-EPR or Fourier transform EPR (FT-EPR), we have realized that the relevant filling factor has not yet been treated in these types of experiments. This might be due to the fact that pulsed-EPR is relatively new and has not been employed much in quantitative work on magnetization measurements. It is noteworthy that pulsed-NMR, although much more mature, still uses the conventional CW filling factor definitions, mainly because of the fact that the wavelength is much larger than the dimensions of the 'cavity' used, and thus the fields, in term of magnitude and phase, are rather homogenous. In EPR, however, the cavity's dimensions are larger than the wavelength, and variations of field amplitudes and phases must be considered as well. It is evident, therefore, that the CW treatment cannot be applied to the pulsed case.

Several publications are related to some aspects of signal intensity, which are unique in pulsed experiments. Based on the amplitude of the magnetization generated in the xy plane, Bowman [8] has treated the case of signal intensity in pulsed EPR, by taking into account the pulse length and microwave frequency. His method can be applied to many pulse sequences in a general way, by employing the Jaynes [9] and Bloom [10] treatment in NMR experiments. However, Bowman's approach lacks the relationship between the position of the xy magnetization in the cavity to the efficiency of it's coupling to the detector outside the cavity. This point shall be further clarified in the next chapter. Recent publication by Eaton and co-workers [11] calculated the EPR signal intensity obtained in a two-pulse Hahn echo experiment. The later treatment is very accurate and takes into account both the xy magnetization distribution and the coupling of this magnetization to the detector. Nevertheless, their study is restricted to the two-pulse Hahn echo experiment, without elaborating on the difference between the pulsed- and CW-EPR methods.

Recently, we have developed an experimental method, which requires the evaluation of the relative contributions to the overall pulsed-EPR signal intensity from different parts of a sample in a rectangular cavity [5,12]. The detailed treatment of the problem discussed in Ref. [12] is presented here. It is an extension of the studies described in Refs. [8,11] and is based on a new approach, which can be applied to the most common pulse sequences. In particular, it is useful in many light-induced FT-EPR experiments. This method allows one to evaluate the signal intensity via the filling factor (η_p), described in this paper, in a pulsed experiment. We will present some examples, which will better clarify the difference between CW and pulsed-EPR filling factors.

2. Filling factor in pulsed-EPR experiments

Every pulse experiment consists of at least two stages: (a) excitation by a particular pulse sequence; and (b) free induction decay (FID) or echo detection. In the first stage, magnetization is created in the xy plane in the laboratory frame (where the z-axis is the direction of the DC magnetic field), and in the second stage, the precessing magnetization in the xy plane, M_{xy}, generates magnetic fields, which induce a voltage in the detector. For such an experimental setup an analogous term to the filling factor in the CW case should be considered. The pulsed-EPR filling factor should be a proportional parameter, which is specific for sample geometry and dielectric properties. Therefore, the pulsed-EPR signal intensity following a pulse sequence should be reflected by η_p. In other words, we would like to present an analogous expression to Eq. (2), which should be applicable to the pulsed-EPR case. With respect to the two stages in each pulsed-EPR experiment mentioned above, we can divide η_p calculation into two parts, namely excitation and detection. Following a specific pulse sequence in the first part, we must calculate the amount of precessing magnetization in the xy plane of the laboratory frame of reference. This oscillating

magnetization will probably vary along the sample. For example, in a one-pulse experiment, the FID signal results from the oscillating magnetization in the cavity. Because of the inhomogeneous microwave field along the sample, different parts of the sample will experience different flip angles, and the oscillating magnetization will differ along the sample. In the second part, we must evaluate the signal at the detector induced by M_{xy}. Again, it is evident that if we take the same amount of rotating magnetization and place it first at the center of the cavity, and then near the cavity's walls, a much smaller voltage will be generated in the detector in the later case.

In the first part, we evaluate M_{xy} at different parts along the sample. The distribution of M_{xy} in the sample depends on the specific pulse sequence used, and should be calculated accordingly. In order to present simple and closed form expressions, the calculation of M_{xy} is made with several simplified assumptions for the pulsed case. For example, in a single pulse FID experiment, employing a rectangular cavity (Fig. 1), we can estimate the rotating magnetization distribution as:

$$M_{xy}(x', y', z') = M_0^{\mathrm{FID}} \cdot \sin\theta, \tag{3}$$

where θ is the flip angle between the total magnetization vector $\boldsymbol{M}$ and the laboratory z-axis, given by:

$$\theta = \frac{H_{1x'}(x', y', z')}{H_{1x'}^{\max}} \frac{\pi}{2}, \tag{4}$$

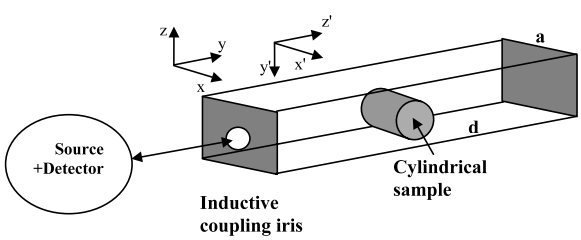

Fig. 1. A rectangular cavity for pulsed-EPR experiments. The xyz coordinate system is the laboratory frame of reference, where z is the direction of the external magnetic field, and $x'y'z'$ is the conventional frame of reference for a rectangular EPR cavity. The dimension of the cavity along the x'-axis is a, and the dimension of the cavity along the z'-axis is d.

where $H_{1x'}^{\max}$ is the microwave magnetic field at the center of the cavity, which is assumed to correspond exactly to a $\pi/2$ pulse. Eq. (4) is exact for on-resonance excitation. It is also a very good approximation for off-resonance excitation in FT-EPR experiments where the spectrum is narrow. If we assume that the magnetic fields in the cavity do not change with sample insertion, we can combine Eqs. (3) and (4) and use the analytical expression for $H_{x'}$ inside the cavity, [13] to obtain:

$$M_{xy}(x', y', z') = M_0^{\mathrm{FID}} \cdot \sin\left\{\sin\left(\frac{\pi x'}{a}\right)\cos\left(\frac{2\pi z'}{d}\right)\frac{\pi}{2}\right\}, \tag{5}$$

where M_0^{FID} is the absolute value of the total magnetization at equilibrium, and a and d are the cavity's dimensions (Fig. 1). It is noteworthy that in these calculations we assume the existence of a homogenous sample with respect to spin concentration. For on-resonance, or near-resonance single pulse excitation along the laboratory x-axis, M_{xy} will lie along the y-axis only, but may exhibit different phases, i.e. it can be negative or positive.

The same approach can be applied to the case in which M_{xy} is a consequence of a two pulse sequence, e.g. Hahn echo. In such a case, the refocused echo magnetization along the y-axis will be [11]:

$$M_{xy}(x', y', z') = M_0^{\mathrm{echo}} \cdot \sin^3\left(\frac{H_{1x'}(x', y', z')}{H_{1x'}^{\max}}\frac{\pi}{2}\right), \tag{6}$$

and again, as in Eq. (5), by assuming no change in the magnetic fields due to the sample insertion, we obtain:

$$M_{xy}(x', y', z') = M_0^{\mathrm{echo}} \cdot \sin^3\left\{\sin\left(\frac{\pi x'}{a}\right)\cos\left(\frac{2\pi z'}{d}\right)\frac{\pi}{2}\right\}. \tag{7}$$

The above examples provide a simplified calculation of M_{xy} distribution along the sample volume. In general, the flip angle in a specific position should be calculated numerically by taking into account the magnitude of the magnetic fields at each point in the cavity, with the sample inserted in it [5]. In most pulse sequences, the method of Jaynes [8,9] can be used to have the

exact expressions for M_{xy}. In more complex spin systems, a full density matrix approach should be employed [14], taking into account that M_{xy} is a complex number with an out-of-phase magnetization along the x-axis.

Following the excitation part treated above, we shall now discuss the detection part, which involves the calculation of the EPR signal from the precessing magnetization, in the laboratory xy plane, where M_{xy} is placed at various sites inside the cavity. In terms of the electromagnetic problem to be solved, we consider a rotating magnetic unit dipole source in an empty cavity, which radiates inside and outside the cavity [15]. The rotating dipole induces local oscillating magnetic fields, which propagate towards the detector. These local fields can be represented as two linear sources, one along the cavities x'-axis and one along the cavities z'-axis, whose intensities are out-of-phase by $\pi/2$ (notice that the magnetization precesses in the $x'z'$ plane).

In order to estimate the relative contribution to the signal at the detector from the precessing magnetization at various parts of the cavity, we will use the reciprocity theorem of electromagnetic fields [16]. Briefly, this theorem states that if a certain voltage source, at point A, generates fields at a point B, then by removing the source, the fields at point B will generate the same voltage as the original source at point A[1]. Thus, in order to complete our second part of calculating η_p, we must first calculate the magnetic fields inside the cavity with the sample inserted in it [5]. These magnetic fields vary in magnitude and phase along the sample. Using the reciprocity theorem, we can deduce that the different magnetic fields we have calculated represent exactly the different weights, with respect to the voltage that a precessing magnetization generates in the detector. This treatment must be applied to each point in the sample. Thus, assuming there is a homogenous equal distribution of rotating M_{xy} in the entire sample volume, the voltage (i.e. the EPR signal) in a linear receiver will be proportional to:

$$S_{\mathrm{EPR}} \propto \left| \int_{V_s} (H_{1x'}(x', y', z') + H_{1z'}(x', y', z')\, e^{i\pi/2})\, dV \right|, \tag{8}$$

where the magnetic fields in the integral are those induced by a source outside the cavity while the sample is inserted.

Eq. (8) assumes a homogeneous precessing magnetization of unit value over the entire sample volume. In practice, M_{xy} distribution in not homogeneous and Eq. (8) should be modified to include this inhomogeneity (Eqs. (5) and (7)). In such a case, the normalized expression with respect to the maximum magnetic field, magnetization, and sample volume is:

$$S'_{\mathrm{EPR}} \propto \eta_p = \frac{\left| \int_{V_s} (H_{1x'}(x', y', z') + H_{1z'}(x', y', z')\, e^{i\pi/2})\, M_{xy}(x', y', z')\, dV \right|}{H_1^{\max} M_{xy}^{\max} V_s}, \tag{9}$$

where we have divided our answer by the maximum magnetic field, magnetization and sample volume to obtain a dimensionless factor.

The integral in Eq. (9) can only be solved numerically. Nevertheless, we can write down a closed-form expression for the various pulse sequences, assuming that the magnetic fields do not change with sample insertion into the cavity. Substituting in Eq. (9) the analytical expressions for $H_{1x'}$ and $H_{1z'}$ [13] and M_{xy} (Eq. (5)) gives the following equation for η_p in the case of a one-pulse FID experiment:

$$\eta_p = \frac{1}{V_s} \left| \int_{V_s} \left\{ \frac{1}{[1+(d/2a)^2]^{1/2}} \sin\left(\frac{\pi x'}{a}\right) \cos\left(\frac{2\pi z'}{d}\right) + \frac{1}{[1+(2a/d)^2]^{1/2}} \cos\left(\frac{\pi x'}{a}\right) \sin\left(\frac{2\pi z'}{d}\right) e^{i\pi/2} \right\} \sin\left\{ \sin\left(\frac{\pi x'}{a}\right) \cos\left(\frac{2\pi z'}{d}\right) \frac{\pi}{2} \right\} dV \right| \tag{10}$$

A similar expression can be obtained for the 2-pulse Hahn echo or any other pulse sequences.

[1] An example of this principle applied in magnetic resonance is the energy of two interacting magnetic dipoles (the dipolar interaction).

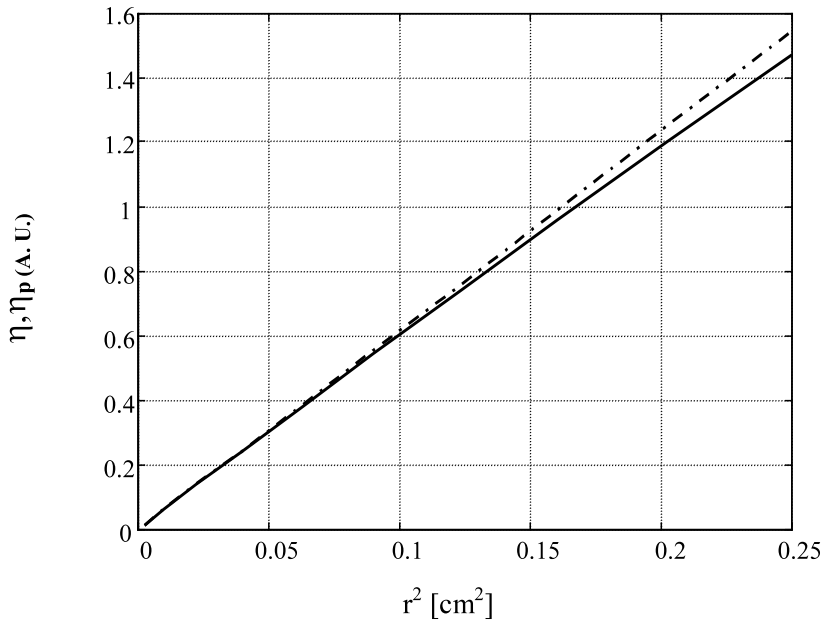

Fig. 2. Functional dependence of η (dashed) and of η_p (solid) upon sample radius (r^2). The filling factor increases with sample size. The numerical calculation of η_p was carried out by employing our recently published algorithm [5] combined with Eq. (9). The dashed line represents an r^2 linear dependence, which corresponds to the CW case [2].

When the unperturbed fields' approximation due to sample insertion does not hold, one should carry out a numerical calculation to determine the electromagnetic fields inside the cavity with the sample-inserted [5]. It should be noted that even in more complex pulse sequences, the same algorithm for η_p still holds and Eq. (9) should be used with a quantum mechanical calculation of M_{xy} [14], as discussed above.

There are several important differences, between the filling factors obtained for the CW- and pulsed-EPR experiments. In the CW case (for critically coupled cavity), η is a normalized and dimensionless figure ranging between 0 and 1, which increases monotonously as the sample size increases. On the other hand, η_p cannot be normalized to be within the range 0–1, and its magnitude is dependent on the coupling parameters of the cavity. Moreover, it does not necessarily increases monotonously; different regions of the sample may contribute to the signal with opposite phases, with the net result of reducing the signal at the detector. An additional important aspect of η_p is that it does not obey Eq. (2). For example, a decrease in the Q-factor of the cavity will not necessarily result in a decrease in the EPR signal. This is due to the fact that the coupling between the cavity and the waveguide may also change; e.g. in the case of overcoupling, the signal may increase.

An important factor, which should be considered in the calculation of η_p, is the possibility of non-ideal pulses. Non-ideal pulses may result, for example, in a situation where the angle of flipping for a $\pi/2$ pulse is more than 90° in the center of the cavity. This would therefore, result in an error in the calculation of η_p, and most of the signal would arise from the peripheral sections of the cavity rather than from the center of the cavity. Thus, there is considerable importance of accurate setting of the cavity for exact angle flipping at the center using point-like sample.

We shall provide the reader with an example regarding the differences between η and η_p with respect to changes in the sample size. It has been shown [2] that when $2a = d$, η for the CW case can be expressed in a closed form where it is proportional to the sample volume, i.e. r^2. Fig. 2 shows η_p for a single pulse FID experiment, as a function

of r^2 (sample radius). The calculation was performed by employing Eq. (10) for X-band frequency and cavity's dimensions of $2a = d = 7$ cm. Inspection of the curves indicate that because of the destructive interference effect, $\eta_p < \eta$, particularly for large values of r^2. In a multi-pulse sequence, the difference between η and η_p increases. In addition to the above arguments, we should also consider the relative contribution of different sample points along the x-axis. As the number of pulses in the sequence increases, the relative contribution of the 'peripheral' regions of the sample to the relevant EPR signal is reduced substantially. This is different from the CW-case, where the contributions from different regions of the sample are nearly fixed and do not drop as fast as we move from the center of the cavity. This case is exemplified in Figs. 3 and 4. It can be seen that for a single pulse sequence, the relative importance of the 'peripheral' sites on the sample with respect to the overall EPR signal is even greater than in the CW case. However, the more pulses employed in the sequence, the less important these peripheral sections become. It is also noted that the differences between η and η_p are small in the center of the sample.

3. Conclusions

We have presented a definition of η_p and its mathematical derivation in a pulsed-EPR experiment. Although we have mainly concentrated on rectangular EPR cavities, the method can be applied to any cavity. This factor depends on quite a few parameters, which exceed those in the CW case, and therefore, is much less 'universal' in its definition and calculation. For example, η_p depends upon the specific pulse sequence employed and the matching parameters of the cavity, factors that are not relevant for the CW-EPR case. Nevertheless, η_p is important for calculation of the

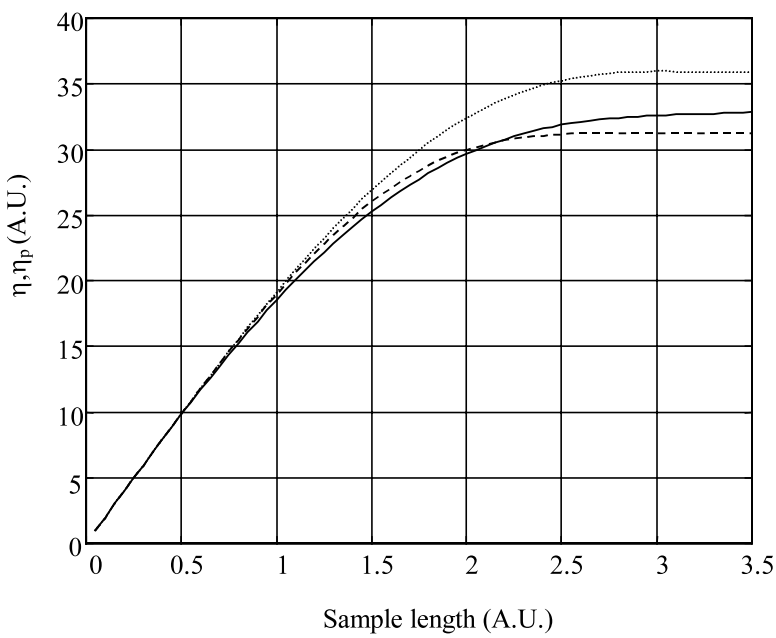

Fig. 3. Numerical calculation of the signal intensity as a function of sample length (for a radius of 2.5 mm, in a rectangular cavity). The calculation was carried out for CW-EPR [2] and two different pulsed-EPR experiments, using Eq. (9). All lines show a saturation effect due to the small contribution of the outer parts of the sample to the EPR signal. CW-EPR (solid line, η), single pulse FID (dotted line, η_p), and two-pulse Hahn echo (dashed line, η_p) are shown. Notice that as the pulse sequence is more complex, the relative contribution from upper and lower parts of the inserted sample is decreased. This feature is important for the evaluation of the relative contribution from irradiated and non-irradiated parts of the sample in an optical excitation experiment [12].

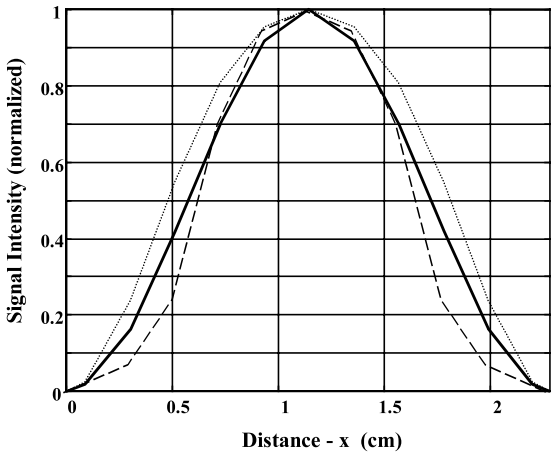

Fig. 4. Numerical calculation of the signal intensity as a function of distance along the sample assuming uniform spin distribution. The calculation was carried out for CW-EPR [2] and different pulsed-EPR experiments (using Eq. (9)). CW-EPR (solid line) exhibits a $\cos^2 x$ dependence. Single pulse FID case (dotted line) and two-pulse Hahn echo case (dashed line) are shown. Magnetic fields calculations were carried out by a full numerical solution of the Maxwell equations [5] for a quartz tube of 2.8 mm i.d. and 4 mm o.d. in an X-band cavity. See also comments in Fig. 3. This type of calculation is important for the evaluation of the relative contribution from lit and unlit parts of the sample in an optical excitation experiment [12].

relative contribution of different regions in the sample to the overall EPR signal and for the comparison between different samples under the same cavity's conditions. These considerations are of prime importance in the analysis of light-induced FT-EPR experiments where the laser beam illuminates only part of the sample [12].

Acknowledgements

This work is in partial fulfillment of the requirements for a Ph.D. degree (A.B.) at the Hebrew University of Jerusalem. This work was partially supported by the Israel Ministry of Science, through the 'Eshkol Foundation Stipends' (A.B.), and by a US–Israel BSF grant and by the Volkswagen Foundation (1/73 145). The Farkas Research Center is supported by the Bundesministerium für die Forschung und Technologie and the Minerva Gesellschaft für Forchung GmbH, FRG. The helpful comments of M.K. Bowman are greatly acknowledged.

References

[1] G. Feher, Bell Systems Technical Journal 36 (1957) 449.
[2] C.P. Poole Jr., Electron Spin Resonance, 2nd ed., Wiley-Interscience, New York, 1983, p. 382.
[3] P. Hedving, Acta Phys. Hungaricae 10 (1959) 115.
[4] G. Casteleijn, J.J. Ten Bosch, J. Smitdh, Journal of Applied Physics 39 (1968) 4375.
[5] A. Blank, H. Levanon, Spectrochimica Acta A 56 (2000) 363.
[6] N.D. Yordanov, P. Slavov, Applied Magnetic Resonance 10 (1996) 351.
[7] R. Czoch, Applied Magnetic Resonance 10 (1996) 293.
[8] M. Bowman, Modern Pulsed and Continuous-Wave Electron Spin Resonance, Wiley, New York, 1990, p. 28.
[9] E. Jaynes, Physical Review 98 (1955) 1099.
[10] A. Bloom, Physical Review 98 (1955) 1105.
[11] G. Rinard, R. Quine, R. Song, G. Eaton, S. Eaton, Journal of Magnetic Resonance 140 (1999) 69.
[12] A. Blank, H. Levanon, Journal of Physical Chemistry A 104 (2000) 794.
[13] N. Marcuvitz, Waveguide Handbook, McGraw-Hill, New York, 1951, p. 57.
[14] D. Gamliel, H. Levanon, Stochastic Processes in Magnetic Resonance, World Scientific, Singapore, 1995, p. 282.
[15] D.I. Hoult, B. Bhakar, Concepts in Magnetic Resonance 9 (1997) 277.
[16] J.D. Krauss, Antennas, 2nd ed., McGraw Hill Book Company, New York, 1988, p. 410.